frontiers in Materials

ORIGINAL RESEARCH
published: 19 May 2015
doi: 10.3389/fmats.2015.00042

Laser patterning of non-linear optical $Bi_2ZnB_2O_7$ crystal lines in glass

*Taisuke Inoue, Xuyi Gao, Kenji Shinozaki, Tsuyoshi Honma and Takayuki Komatsu**

Department of Materials Science and Technology, Nagaoka University of Technology, Nagaoka, Japan

Bi_2O_3-based glasses are very attractive from the viewpoints of low-melting, high refractive index, and crystallization, and the research on their glasses and glass-ceramics is at the frontiers of glass science and technology. Non-linear optical $Bi_2ZnB_2O_7$ crystal lines with a high orientation were patterned in $3Sm_2O_3$-$30.3Bi_2O_3$-33.3ZnO-$33.3B_2O_3$ glass by using a laser-induced crystallization technique. It was confirmed from transmission electron microscope observations that crystals were formed in the inside of the glass, i.e., at the beneath of 4 μm from the surface, although lasers (Yb:YVO_4 laser with a wavelength of 1080 nm) were focused at the glass surface. A new potential for optical device applications was added in Bi_2O_3-based glasses from the present study.

Keywords: bismuth based glass, non-linear optical crystal, laser patterning, crystal orientation, glass-ceramics

OPEN ACCESS

Edited by:
Ashutosh Goel, Rutgers-The State University of New Jersey, USA

Reviewed by:
Jeetendra Sehgal, Sterlite Technologies Limited, India
Zhihua Yang, Chinese Academy of Sciences, China

****Correspondence:***
Takayuki Komatsu, Department of Materials Science and Technology, Nagaoka University of Technology, 1603-1 Kamitomioka-cho, Nagaoka 940-2188, Japan
komatsu@mst.nagaokaut.ac.jp

Specialty section:
This article was submitted to Glass Science, a section of the journal Frontiers in Materials

Received: *20 January 2015*
Accepted: *04 May 2015*
Published: *19 May 2015*

Citation:
Inoue T, Gao X, Shinozaki K, Honma T and Komatsu T (2015) Laser patterning of non-linear optical $Bi_2ZnB_2O_7$ crystal lines in glass. Front. Mater. 2:42. doi: 10.3389/fmats.2015.00042

Introduction

Micro-fabrications in glassy materials have found increasingly more applications in optoelectronics, telecommunications, and photonic devices such as optical gratings and waveguides, and laser irradiation to glasses has received considerable attention as a new tool of spatially selected micro-fabrications in glasses. For instance, a permanent change of refractive index can be induced in Ge-doped SiO_2 optical fibers by using ultraviolet laser irradiations to produce Bragg gratings under suitable exposure conditions. Spatially selected patterning of crystals in glasses by laser irradiations, i.e., laser-induced crystallization, is also extremely attractive, which is a new method for the design and control of the crystallization of glasses in comparison with the conventional crystallization technique using an electric furnace, and also opens a new door in crystal growth and patterning engineering. The design and control of the crystallization of glasses by using lasers are at the frontiers of the glass science and technology.

The present authors group proposed new laser irradiation techniques for the patterning of crystals with dot, line, and two-dimensional planar shapes in glasses, i.e., the rare-earth atom heat (REAH) processing and transition metal atom heat (TMAH) processing (Sato et al., 2001; Honma et al., 2003, 2006; Komatsu et al., 2007; Komatsu and Honma, 2013), and various crystals such as ferroelectric $LiNbO_3$ (Honma and Komatsu, 2010; Komatsu et al., 2011), multi-ferroic β'-$RE_2(MoO_4)_3$ (RE: rare-earth) (Tsukada et al., 2009; Suzuki et al., 2010), non-linear optical $Li_2Si_2O_5$ (Honma et al., 2008), oxyfluoride $BaAlBO_3F_2$ (Shinozaki et al., 2012), and fluoride CaF_2 (Shinozaki et al., 2013) have been patterned successfully in glasses. In the laser-induced crystallization, a steep temperature gradient is created in the laser irradiated local region and such a steep temperature gradient is moved along laser scanning direction, consequently providing the patterning of crystals with a high orientation. It is of very importance to apply the laser-induced crystallization technique to various glasses, and such studies will lead a more deep understanding of the crystallization of glasses and also the possibility of new device applications of crystallized glasses (glass-ceramics).

In this study, we focus our attention on the patterning of non-linear optical $Bi_2ZnB_2O_7$ crystal lines with a high orientation in Bi_2O_3–ZnO–B_2O_3 glasses by using a laser-induced crystallization technique. Recently, $Bi_2MB_2O_7$ crystals (M = Zn, Sr, and Ca) have been successfully synthesized through the crystallization of corresponding glasses (Majhi and Varma, 2008a,b; Kanenishi et al., 2012; Shanmugavelu and Kumar, 2012). In particular, $Bi_2ZnB_2O_7$ with an orthorhombic structure is of interest, because $Bi_2ZnB_2O_7$ exhibits excellent non-linear optical properties (Barbier et al., 2005) and is crystallized from $33.3Bi_2O_3$-33.3ZnO-$33.3B_2O_3$ glass corresponding to the stoichiometric composition of $Bi_2ZnB_2O_7$. The values of second-order optical non-linearities, $d_{31} = 0.911$ pm/V, $d_{32} = 3.083$ pm/V, and $d_{33} = 1.015$ pm/V, have been reported for $Bi_2ZnB_2O_7$ single crystal (Su et al., 2013). Very recently, transparent glass-ceramics containing $Bi_2ZnB_2O_7$ nanocrystals have been synthesized in $30Bi_2O_3$-40ZnO-$30B_2O_3$ glass, and it has been found that they exhibit a large third-order optical non-linearity (Zeng et al., 2014). Furthermore, $Bi_2ZnB_2O_7$ nanocrystals have been patterned in ZnO–Bi_2O_3–B_2O_3 glasses by irradiations of femtosecond laser (Liu et al., 2015). There has been, however, no report on the laser patterning of $Bi_2ZnB_2O_7$ crystal lines (not dots) with a high orientation in glasses so far. In a previous paper (Inoue et al., 2010), we examined the features of electronic polarizability (optical basicity) and chemical bonding state in Bi_2O_3–ZnO–B_2O_3 glasses from density, refractive index, Raman scattering spectrum, and X-ray photoelectron spectrum (XPS) measurements, and proposed the formation of B–O–Bi and B–O–Zn bridging bonds in the glass structure. In this paper, we demonstrated that $Bi_2ZnB_2O_7$ crystal lines with a high orientation were patterned in Bi_2O_3–ZnO–B_2O_3 glasses by laser irradiations for the first time. Glasses based on the Bi_2O_3–ZnO–B_2O_3 system have also received much attention as new low-melting and shielding glasses (Maeder, 2013), and from this point of view, the understanding of the crystallization behaviors of Bi_2O_3–ZnO–B_2O_3 glasses is extremely important. The laser patterning of functional crystals in Bi_2O_3-based glasses has a great potential in application of non-linear optical integrated devices (Liu et al., 2015), and is at the frontiers of glass science and technology in Bi_2O_3-based glasses.

Experimental Section

Glasses with the compositions of $33.3Bi_2O_3$-33.3ZnO-$33.3Bi_2O_3$ and xSm_2O_3-(33.3-x)Bi_2O_3-33.3ZnO-$33.3B_2O_3$ ($x = 1$, 3, and 5) were prepared by using a conventional melt quenching technique. Commercial powders of reagent grade ZnO, Bi_2O_3, H_3BO_3, and Sm_2O_3 were melted in a platinum crucible at 1000°C for 30 min in an electric furnace. The melts were poured onto an iron plate and pressed to a thickness of ~1.5 mm by another iron plate. Glass transition (T_g) and crystallization peak temperatures (T_p) were determined by using differential thermal analysis (DTA) at a heating rate of 10 K/min. The quenched glasses were annealed at T_g for 30 min to release internal stresses. Densities of glasses were determined with the Archimedes method using distilled water as an immersion liquid (Inoue et al., 2010). Refractive indices at a wavelength (λ) of 632.8 nm (He–Ne laser) were measured at room temperature with a prism coupler (Metricon Model 2010). The melt-quenched plate-shaped glasses were heat-treated at some temperatures in an electric furnace, i.e., at 450–530°C for 3 h, and the crystalline phases formed were identified by using X-ray diffraction (XRD) analysis at room temperature. Raman scattering spectra at RT for the glasses and heat-treated samples were measured with a laser microscope (Tokyo Instruments Co., Nanofinder) operated at Ar^+ laser (wavelength: λ = 488 nm). In this apparatus, the data below 250 cm^{-1} cannot be measured due to the use of an edge filter.

Glasses were mechanically polished to a mirror finish with CeO_2 powders. The glass was irradiated by cw Yb:YVO_4 fiber laser (beam shape: single mode and ± 1 nm bandwidth) with λ = 1080 nm using objective lens (magnification: 50 times, numerical aperture: NA = 0.8). The laser beam was unpolarized and the diameter of laser spot was 2~3 μm. Plate-shaped glasses with a thickness of ~ 1 mm were put on the stage and mechanically moved during laser irradiations to pattern crystals. The crystalline phase in the laser-irradiated part was examined from micro-Raman scattering spectrum measurements. Second harmonic generation (SHG) microscopic measurements were performed for the laser-irradiated part using a Q-switched Nd:YAG (yttrium aluminum garnet) laser with λ= 1064 nm as a fundamental light source. SHG emissions (λ= 532 nm) were measured, although the fundamental one must be isolated by a cut-off filter before reaching to the CCD (Charged Coupled Devices) for image detection (Fujiwara et al., 2003). The morphology of crystals in laser-patterned lines were examined by using a transmission electron microscope (TEM: FE-TEM, JEOL, JEM-2100F) operating at 200 kV. Thin foils for TEM observations were prepared with a focused Ga ion beam (FIB) (JEOL, JIB-4500) method.

Results and Discussion

Crystallization Behavior of $33.3Bi_2O_3$-33.3ZnO-$33.3B_2O_3$ Glass

Prior to the laser patterning of $Bi_2ZnB_2O_7$ crystal lines in Bi_2O_3–ZnO–B_2O_3 glasses, it is necessary to confirm the formation of $Bi_2ZnB_2O_7$ crystals in the crystallization of a given glass. Basically, the crystalline phase formed by laser irradiations in glasses is the same as that formed by heat treatments in an electric furnace. The glass with the composition of $33.3Bi_2O_3$-33.3ZnO-$33.3B_2O_3$ corresponding to the stoichiometric composition of the $Bi_2ZnB_2O_7$ crystalline phase is designated here as 111BiZnB glass.

Figure 1 shows the DTA patterns for the bulk and powdered samples of as-quenched 111BiZnB glasses. In both samples, endothermic dips due to the glass transition and exothermic peaks due to the crystallization are detected clearly, providing the values of $T_g = 395$°C and $T_p = 562$°C for the bulk sample and $T_g = 395$°C and $T_p = 551$°C for the powdered sample. It is noted that the crystallization peak temperature ($T_p = 562$°C) for the bulk sample is close to that ($T_p = 551$°C) for the powdered sample, implying the possibility of the so-called bulk crystallization in the inside of glass. In **Figure 1**, the optical microscope photograph for the base glass is included. The glass is colorless in the visible region. The density (d) and refractive index (n) of 111BiZnB glass at room temperature are $d = 6.53$ g/cm^3 and $n = 2.06$, respectively.

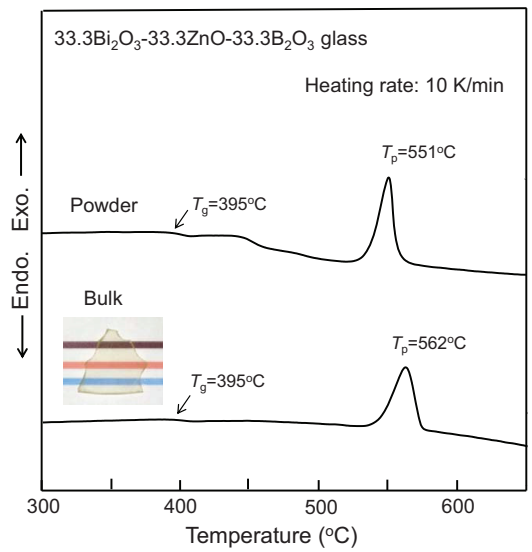

FIGURE 1 | DTA patterns for the bulk and powdered samples of as-quenched glass. T_g and T_p are the glass transition and crystallization peak temperatures, respectively. Heating rate was 10 K/min. The optical microscope photograph for the base glass is included.

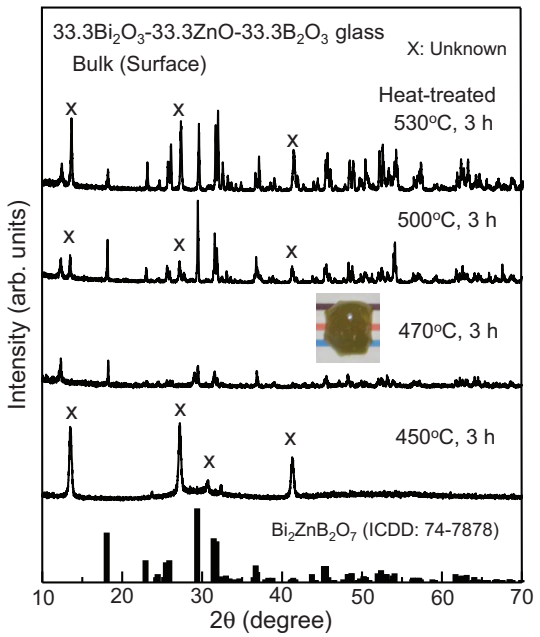

FIGURE 2 | XRD patterns at room temperature for the bulk (i.e., surface) samples obtained by different heat treatment temperatures for 3 h in air. The optical microscope photograph for the sample heat-treated at 470°C is included.

Figure 2 shows the XRD patterns at room temperature for the 111BiZnB samples obtained by different heat treatment temperatures for 3 h in air. In these XRD measurements, the bulk samples were used without any pulverizing and thus information on the crystalline phase being present at and near the glass surface is obtained. As seen in **Figure 2**, the formation of $Bi_2ZnB_2O_7$ crystals is confirmed in the samples heat-treated at 470, 500, and 530°C. Another crystalline phase is formed initially, which has not been identified (i.e., unknown crystalline phase) in our study. It has been reported that the β-BiB_3O_6 crystalline phase is formed initially in the crystallization of 111BiZnB glass (Shanmugavelu and Kumar, 2012). In **Figure 2**, the optical microscope photograph for the sample heat-treated at 470°C is included. It is seen that the surface of the bulk sample is rounded. This behavior indicates that the softening/deformation of samples and crystallization occur almost simultaneously during heat treatments in 111BiZnB glass (Kanenishi et al., 2012). The high thermal stability against the crystallization in 111BiZnB glass, i.e., $\Delta T = T_p - T_g = 562°C - 395°C = 167°C$, would be one of the reasons for the sample deformation during heat treatments. As seen in **Figure 2**, the formation of unknown crystalline phase is detected in the sample heat-treated at 450°C from the XRD pattern; but in the sample heat-treated at 470°C, the formation of such an unknown crystalline phase is not confirmed. The crystallization at the glass surface is influenced by various factors such as surface quality, tips, cracks and scratches, foreign particles, and surrounding atmosphere in a given glass, i.e., the surface state (Müller et al., 2000). The shape of the sample heat-treated at 470°C was changed, i.e., the rounded shape (see **Figure 2**). This means that the surface state is largely changed in the heat treatment at 470°C, and thus the surface crystallization behavior would be influenced, providing the formation behavior of the unknown crystalline phase.

Figure 3 shows the XRD patterns at room temperature for the powdered samples, in which bulk plate-shape glasses were heat-treated and the samples were pulverized after heat treatments. **Figure 3** provides, therefore, information mainly on the crystalline phase present in the interior of samples. All XRD peaks in **Figure 3** are assigned to the $Bi_2ZnB_2O_7$ crystalline phase (ICDD: 74–7878), indicating that only the $Bi_2ZnB_2O_7$ crystalline phase is formed in all samples heat-treated at 450–530°C for 3 h in air. SHGs were confirmed in the crystallized samples (data are not shown here), indicating that the $Bi_2ZnB_2O_7$ crystalline phase formed in 111BiZnB glass exhibits the second-order optical non-linearity. **Figure 4** shows the Raman scattering spectra at room temperature for the base glass and crystallized (530°C, 3 h) samples. The glass shows very broad peaks being typical for glassy materials in the Raman scattering spectrum, i.e., at ~350, ~600, ~920, 1150 ~ 1400, and ~1550 cm^{-1}. From the Raman scattering spectra for various Bi_2O_3–ZnO–B_2O_3 glasses such as $30Bi_2O_3$-30ZnO-$40B_2O_3$, the formation of B–O–Bi and B–O–Zn bridging bonds in the glass structure has been proposed (Inoue et al., 2010). The broad peaks observed in **Figure 4** would be assigned as follows: (1) the band at 350 cm^{-1} can be connected with a symmetric stretching motion in Bi–O–Bi bonds between BiO_6 groups; (2) the band at 600 cm^{-1} could be assigned to symmetric stretching motions in B–O–Bi and B–O–Zn bonds; (3) the band at 920 cm^{-1} can be related mainly to asymmetric stretching motions in B–O–Bi and B–O–Zn bonds; (4) the bands at 1150 ~ 1400 and ~1550 cm^{-1} can be assigned to an asymmetric stretching vibration of B–O bonds in BO_3 groups. On the other hand, the crystallized sample shows several sharp peaks at 347, 382, 497, 537, 577, 632, 699, and 741 cm^{-1} together

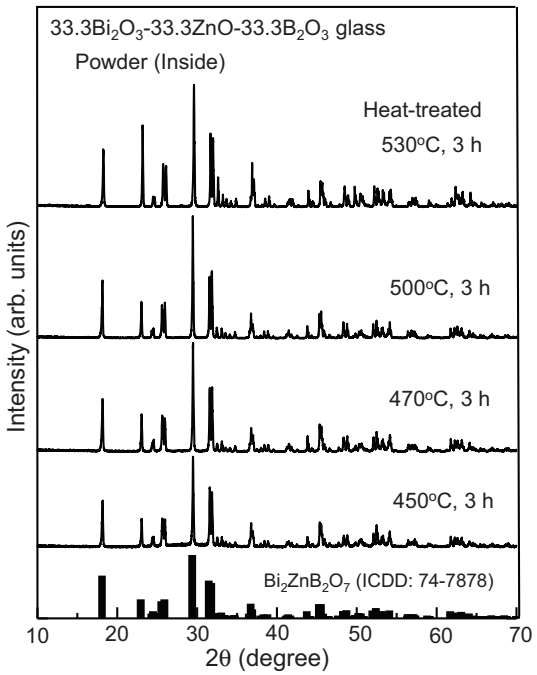

FIGURE 3 | XRD patterns at room temperature for the powdered (i.e., inside) samples obtained by different heat treatment temperatures for 3 h in air. All XRD peaks are assigned to the $Bi_2ZnB_2O_7$ crystalline phase (ICDD: 74–7878).

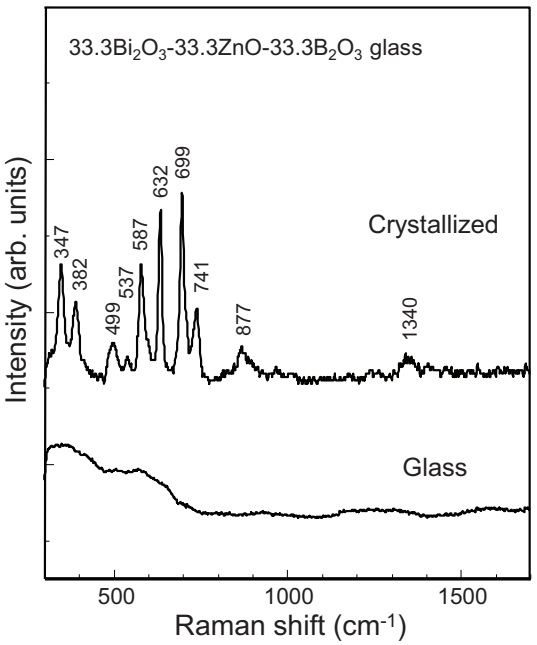

FIGURE 4 | Raman scattering spectra at room temperature for the base glass and crystallized (530°C, 3 h) samples.

with broad and weak peaks at 877, 1243, 1340, and 1548 cm^{-1}. Because $Bi_2ZnB_2O_7$ crystals are formed in the crystallized sample, it is obvious that the Raman scattering spectrum shown in **Figure 4** is for the $Bi_2ZnB_2O_7$ crystalline phase. In $Bi_2ZnB_2O_7$ with an orthorhombic structure ($a = 1.0827$ nm, $b = 1.10329$ nm, and $c = 0.48848$ nm) (Barbier et al., 2005), octahedral BiO_6 units, tetrahedral ZnO units, BO_3 and BO_4 units are present. ZnO_4 units and BO_3/BO_4 units are connected through a corner-shared bonding, i.e., the presence of B–O–Zn bonds, and are creating layers. The $Bi_2ZnB_2O_7$ crystalline phase is, therefore, constructed from the stacking of BiO_6, ZnO_4, BO_3, and BO_4 units. At this moment, the peaks shown in **Figure 4** have not been assigned in detail. However, the Raman scattering spectrum for $Bi_2ZnB_2O_7$ crystals would be used for the confirmation of the presence of $Bi_2ZnB_2O_7$ crystals in laser-patterned lines.

Laser Pattering of $Bi_2ZnB_2O_7$ Crystal Lines

In the laser-induced crystallization technique proposed and applied by our group (Komatsu et al., 2007; Komatsu and Honma, 2013), some amounts of rare-earth ions such as Sm^{3+} or transition metal ions such as Ni^{2+} must be included into the base glass for the absorption of laser. In this study, the glasses with the compositions of xSm_2O_3-(33.3-x)Bi_2O_3-33.3ZnO-33.3B_2O_3 ($x = 1$, 3, and 5) were prepared. The melt-quenched samples with these compositions were confirmed to be glasses from XRD and DTA measurements.

For the glass with $1Sm_2O_3$ ($x = 1$), it was found that laser irradiations with different conditions such as the laser powers of $P = 1.3$–1.5 W and the laser scanning speed of $S = 1.5$ μm/s did not induce any crystallization. Furthermore, for the glass with $5Sm_2O_3$ ($x = 5$), it was difficult to pattern crystal lines with a homogeneous morphology. Here, therefore, the results for the glass with $3Sm_2O_3$ ($x = 3$), i.e., $3Sm_2O_3$-30.3Bi_2O_3-33.3ZnO-33.3B_2O_3 (designated here as 3Sm-111BiZnB glass) are presented. The 3Sm-111BiZnB glass has the values of $T_g = 410$°C and $T_p = 553$°C. Because of the substitution of Sm_2O_3 for Bi_2O_3, the glass transition temperature is becoming high and the crystallization temperature is low compared with the 111BiZnB glass ($T_g = 395^\circ$C and $T_p = 562^\circ$C) with no Sm_2O_3. The value of the optical absorption coefficient (α) at $\lambda = 1080$ nm (Yb:YVO_4 laser) was $\alpha = 10.5\ cm^{-1}$ for 3Sm-111BiZnB glass. The reflection of light at the glass surface calculated using the Fresnel's equation was considered in the estimation of α (i.e., Lambert–Beer law).

Figure 5 shows the polarized optical microphotographs (POMs) for the samples obtained by laser irradiations. The laser scanning speed was fixed to $S = 1.5$ μm/s, and the laser power was changed in the range of $P = 1.30$–1.50 W. The laser was focused at the surface (not in the inside). The lines patterned with $P = 1.30$–1.45 W show a homogeneous distribution in color along the laser scanning direction, indicating that a stable structural change is taking place under these laser irradiation conditions. The morphology of the line patterned with $P = 1.50$ W is not homogeneous. **Figure 6** shows the micro-Raman scattering spectra at room temperature for the lines patterned by laser irradiations with $P = 1.35$ and 1.50 W. In both lines, several sharp peaks are observed and the positions of these peaks are almost similar to the $Bi_2ZnB_2O_7$ crystalline phase (**Figure 4**), indicating that the lines patterned with $P = 1.35$ and 1.50 W consist of $Bi_2ZnB_2O_7$ crystals. In **Figure 6**, the SHG microscopy images of these lines are presented, indicating that SHG emissions are founded to be

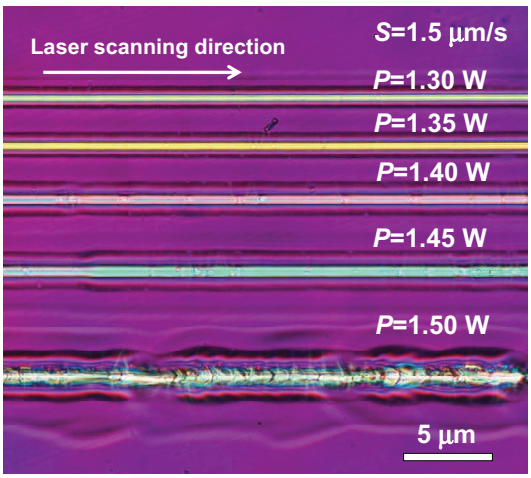

FIGURE 5 | Polarized optical microphotographs for the samples obtained by laser irradiations with the laser powers of $P = 1.3$–1.5 W and a laser scanning speed of $S = 1.5$ μm/s.

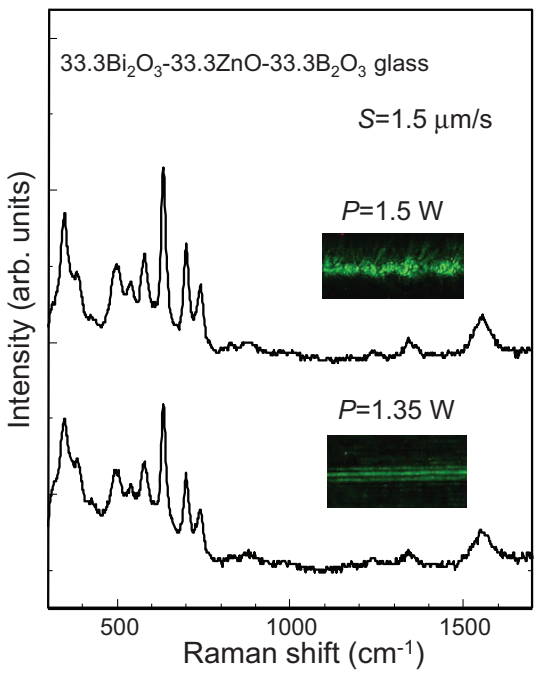

FIGURE 6 | Micro-Raman scattering spectra at room temperature for the lines patterned by laser irradiations with $P = 1.35$ and 1.50 W.

caused by only the crystal lines. Similar results were obtained for other lines patterned with $P = 1.30$, 1.40, and 1.45 W.

In order to examine the morphology and orientation of $Bi_2ZnB_2O_7$ crystals in the line patterned by laser irradiations with $S = 1.5$ μm/s and $P = 1.35$ W by using TEM observations, the line part was processed to a thin foil (~100 nm) shape using a FIB method. **Figure 7** shows the bright field image and selected area electron diffraction (SAED) pattern in TEM observations for the cross-section of the line. Almost a homogeneous bright field image is observed over the whole crystallized part. In the

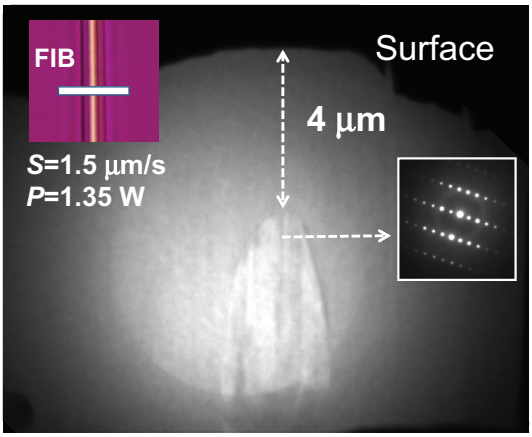

FIGURE 7 | A bright field image and selected area electron diffraction (SAED) pattern in TEM observations for the cross-section of the line patterned by laser irradiations with $S = 1.5$ μm/s and $P = 1.35$ W.

SAED, the diffraction spots are observed clearly. These results suggest that $Bi_2ZnB_2O_7$ crystals in the cross-section (i.e., in the line) are highly oriented, and the line is not constructed from the assembly of $Bi_2ZnB_2O_7$ polycrystals. In order to determine definitely the orientation direction/quality of $Bi_2ZnB_2O_7$ crystals in the lines patterned, further TEM observations are required (Fan et al., 2012). In the present study, the laser focal position was the surface. However, as seen in **Figure 7**, $Bi_2ZnB_2O_7$ crystals were formed in the inside of the glass, i.e., at the beneath of 4 μm from the surface. Usually, if the laser focal position is the surface of a given glass, crystals are basically formed at the glass surface [e.g. Komatsu et al. (2007) and Komatsu and Honma (2013)]. The crystal growth in the inside of the glass (**Figure 7**) observed in this study might be closely related to the high thermal stability (i.e., $\Delta T = T_p - T_g = 167^{\circ}$C) against the crystallization in the glass of $3Sm_2O_3$-$30.3Bi_2O_3$-$33.3ZnO$-$33.3B_2O_3$. As shown in **Figures 2** and **3**, although unknown crystals are formed initially at the glass surface, the main crystalline phase formed in the inside is the $Bi_2ZnB_2O_7$ crystalline phase. This would be one of the reasons for the formation of $Bi_2ZnB_2O_7$ crystals in the lines patterned by laser irradiations. Recently, non-linear optical β-BaB_2O_4 (β-BBO) crystal lines have been successfully patterned in the inside (up to the beneath of ~200 μm) of $8Sm_2O_3$-$42BaO$-$50B_2O_3$ glass by laser irradiations, in which the laser focal position was moved gradually from the surface to the inside (Nishii et al., 2015). The present study suggests that the patterning of $Bi_2ZnB_2O_7$ crystal lines would be possible even in the inside of more deep beneath around 100 μm for Bi_2O_3–ZnO–B_2O_3 glasses by changing the laser focal position.

Frontiers of Laser Pattering of Crystals in Bi_2O_3-Based Glasses

Nowadays, it has been well recognized that Bi_2O_3 oxide is one of the important constituents for the design and control of optical, electrical, and thermal properties of oxide glasses, and numerous studies on Bi_2O_3-based glasses have been studied so far (Dumbaugh, 1986; Maeder, 2013). The most attractive features of Bi_2O_3 oxide are a large electronic polarizability and a weak

single bond strength of Bi–O bonds (Dimitrov and Komatsu, 1999, 2002, 2005, 2010; Komatsu et al., 2010). Indeed, glasses with Bi_2O_3 exhibit large third order non-linear optical susceptibilities $\chi^{(3)}$ of the order 10^{-12} esu (Terashima et al., 1997). Recently, Bi_2O_3–ZnO–B_2O_3 glasses have received much attention (Kim et al., 2007; Doweidar and Saddeek, 2009; Inoue et al., 2010; Hashimoto et al., 2011), in particular, because they are low melting glasses with high thermal stability and have been used as new sealing glasses instead of PbO-containing low melting glasses. The crystallization of Bi_2O_3-based glasses has also received much attention, because some functional crystals containing Bi_2O_3 are formed through the crystallization. For instance, high-T_c Bi_2O_3-based copper superconducting glass-ceramics have been synthesized through the crystallization of glasses with Bi_2O_3 (Komatsu et al., 1988, 1990). Non-linear optical $RE_xBi_{1-x}BO_3$ crystals (RE: Gd and Sm) showing strong SHGs have been also synthesized from RE_2O_3–Bi_2O_3–B_2O_3 glasses (Honma et al., 2002; Ihara et al., 2004; Koshiba et al., 2007). The design and control of new Bi_2O_3-based glasses and their crystallization are at the frontiers of the glass science and technology.

In this study, we demonstrated that non-linear optical $Bi_2ZnB_2O_7$ crystal lines with a homogeneous morphology and a high orientation are patterned in $3Sm_2O_3$-$30.3Bi_2O_3$-$33.3ZnO$-$33.3B_2O_3$ glass for the first time. Crystallized glasses (glass-ceramics) are composites of the glassy phase and crystalline phase, i.e., glass/crystal hybrid materials. In particular, the combination of glass and single crystal line would have a high potential for device applications. It is emphasized that a new potential for optical device applications is added in Bi_2O_3-based glasses from the present study. A large single crystal and crystal fibers of $Bi_2ZnB_2O_7$ have been fabricated in order to develop new solid state lasers with high transparency in the ultra-violet region (Kozhayam et al., 2013; Su et al., 2013). The laser patterning of $Bi_2ZnB_2O_7$ crystal lines in glasses is a new and innovative approach for the single crystal growth technique. Very recently, non-linear optical β-BBO crystal lines with bending and curved shapes have been patterned at the glass surface, and it has been demonstrated from birefringence imaging measurements that highly *c*-axis oriented β-BBO crystals grow along laser scanning direction even if the laser scanning direction changes (Ogawa et al., 2013). As further studies, the patterning of bending and curved $Bi_2ZnB_2O_7$ crystal lines is strongly required in Bi_2O_3–ZnO–B_2O_3 glasses.

Conclusion

Non-linear optical $Bi_2ZnB_2O_7$ crystal lines with a high orientation were patterned in $3Sm_2O_3$-$30.3Bi_2O_3$-$33.3ZnO$-$33.3B_2O_3$ glass by using a laser-induced crystallization technique for the first time, in which continuous-wave Yb:YVO_4 fiber lasers with a wavelength of 1080 nm were irradiated at the glass surface. It was confirmed from transmission electron microscope observations that crystals were formed in the inside of the glass, i.e., at the beneath of 4 μm from the surface. A new potential for optical device applications was added in Bi_2O_3-based glasses from the present study.

Acknowledgments

This work was supported from the Grant-in-Aid for Scientific Research from the Ministry of Education, Science, Sports, Culture and Technology, Japan (No. 23246114) and by Program for High Reliable Materials Design and Manufacturing in Nagaoka University of Technology.

References

Barbier, J., Penin, N., and Cranswick, L. M. (2005). Melilite-type borates $Bi_2ZnB_2O_7$ and $CaBiGaB_2O_7$. *Chem. Mater.* 17, 3130–3136. doi:10.1021/cm0503073

Dimitrov, V., and Komatsu, T. (1999). Electronic polarizability, optical basicity and nonlinear optical properties of oxide glasses. *J. Non Cryst. Solids* 249, 160–179. doi:10.1016/S0022-3093(99)00317-8

Dimitrov, V., and Komatsu, T. (2002). Classification of simple oxides: a polarizability approach. *J. Solid State Chem.* 163, 100–112. doi:10.1006/jssc.2001.9378

Dimitrov, V., and Komatsu, T. (2005). Classification of oxide glasses: a polarizability approach. *J. Solid State Chem.* 178, 831–846. doi:10.1016/j.jssc.2004.12.013

Dimitrov, V., and Komatsu, T. (2010). Average single bond strength and optical basicity of Bi_2O_3-B_2O_3 and Sb_2O_3-B_2O_3 glasses. *J. Non Cryst. Solids* 356, 258–262. doi:10.1016/j.jnoncrysol.2009.11.014

Doweidar, H., and Saddeek, Y. B. (2009). FTIR and ultrasonic investigations on modified bismuth borate glasses. *J. Non Cryst. Solids* 355, 348–354. doi:10.1016/j.jnoncrysol.2008.12.008

Dumbaugh, W. H. (1986). Heavy metal oxide glasses containing Bi_2O_3. *Phys. Chem. Glasses* 27, 119–123.

Fan, C., Poumellec, B., Lancy, M., He, X., Zeng, H., Erraji-Chahid, A., et al. (2012). Three-dimensional photoprecipitation of oriented $LiNbO_3$-like crystals in silica-based glass with femtosecond laser irradiation. *Opt. Lett.* 37, 2955–2957. doi:10.1364/OL.37.002955

Fujiwara, T., Sawada, T., Honma, T., Benino, Y., Komatsu, T., Takahashi, M., et al. (2003). Origin of intrinsic second-harmonic generation in crystallized GeO_2-SiO_2 glass films. *Jpn. J. Appl. Phys.* 42, 7326–7330. doi:10.1143/JJAP.42.7326

Hashimoto, T., Shimada, Y., Nasu, H., and Ishida, A. (2011). ZnO-Bi_2O_3-B_2O_3 glasses as molding glasses with high refractive indices and low coloration codes. *J. Am. Ceram. Soc.* 94, 2061–2066. doi:10.1111/j.1551-2916.2010.04383.x

Honma, T., Benino, Y., Fujiwara, T., Sato, R., and Komatsu, T. (2002). Optical nonlinear crystalline dot and line patterning in samarium bismuth borate glasses by YAG laser irradiation. *J. Ceram. Soc. Jpn.* 110, 398–402. doi:10.2109/jcersj.110.398

Honma, T., Benino, Y., Fujiwara, T., Komatsu, T., and Sato, R. (2003). Nonlinear optical crystal line writing in glass by yttrium aluminium garnet laser irradiation. *Appl. Phys. Lett.* 82, 892–894. doi:10.1063/1.1544059

Honma, T., Benino, Y., Fujiwara, T., and Komatsu, T. (2006). Transition metal atom heat processing for writing of crystal lines in glass. *Appl. Phys. Lett.* 88, 231105. doi:10.1063/1.2212272

Honma, T., and Komatsu, T. (2010). Patterning of two-dimensional planar lithium niobate architectures on glass surface by laser scanning. *Opt. Express* 18, 8019–8024. doi:10.1364/OE.18.008019

Honma, T., Nguyen, P. T., and Komatsu, T. (2008). Crystal growth behavior in CuO-doped lithium disilicate glasses by continuous-wave fiber laser irradiation. *J. Ceram. Soc. Jpn.* 116, 1314–1318. doi:10.2109/jcersj2.116.1314

Ihara, R., Honma, T., Benino, Y., and Komatsu, T. (2004). Second-order optical nonlinearities of metastable $BiBO_3$ phases in crystallized glasses. *Opt. Mater.* 27, 403–408. doi:10.1016/j.optmat.2004.07.002

Inoue, T., Honma, T., Dimitrov, V., and Komatsu, T. (2010). Approach to thermal properties and electronic polarizability from average single bond strength in ZnO-Bi_2O_3-B_2O_3 glasses. *J. Solid State Chem.* 183, 3078–3085. doi:10.1016/j.jssc.2010.10.027

Kanenishi, K., Sakida, S., Benino, Y., and Nanba, T. (2012). Surface crystallization of stoichiometric glass with $Bi_2ZnB_2O_7$ crystal using ultrasonic surface treatment

followed by heat treatment. *J. Ceram. Soc. Jpn*. 120, 509–512. doi:10.2109/jcersj2.120.509

Kim, B. S., Lim, E. S., Lee, J. H., and Kim, J. J. (2007). Effect of structure change on thermal and dielectric characteristics in low-temperature firing Bi_2O_3-B_2O_3-ZnO glasses. *J. Mater. Sci.* 42, 4260–4264. doi:10.1007/s10853-006-0638-y

Komatsu, T., Sato, R., Imai, K., Matusita, K., and Yamashita, T. (1988). High-T_c superconducting glass ceramics based on the Bi-Ca-Sr-Cu-O system. *Jpn. J. Appl. Phys.* 27, L550–L552. doi:10.1143/JJAP.27.L533

Komatsu, T., Hirose, C., Ohki, T., Sato, R., and Matusita, K. (1990). Preparation of Ag-coated superconducting $Bi_2Sr_2CaCu_2O_x$ glass ceramic fibers. *Appl. Phys. Lett.* 57, 183–185. doi:10.1063/1.103978

Komatsu, T., and Honma, T. (2013). Laser patterning and characterization of optical active crystals in glasses (review). *J. Asian Ceram. Soc.* 1, 9–16. doi:10.1016/j.jascer.2013.02.006

Komatsu, T., Ihara, R., Honma, T., Benino, Y., Sato, R., Kim, H. G., et al. (2007). Patterning of nonlinear optical crystals in glass by laser-induced crystallization. *J. Am. Ceram. Soc.* 90, 699–705. doi:10.1111/j.1551-2916.2006.01441.x

Komatsu, T., Ito, N., Honma, T., and Dimitrov, V. (2010). Electronic polarizability and its temperature dependence of Bi_2O_3-B_2O_3 glasses. *J. Non Cryst. Solids* 356, 2310–2314. doi:10.1016/j.jnoncrysol.2010.03.041

Komatsu, T., Koshiba, K., and Honma, T. (2011). Preferential growth orientation of laser-patterned $LiNbO_3$ crystals in lithium niobium silicate glass. *J. Solid State Chem.* 184, 411–418. doi:10.1016/j.jssc.2010.12.016

Koshiba, K., Honma, T., Benino, Y., and Komatsu, T. (2007). Patterning and morphology of nonlinear optical $Gd_xBi_{1-x}BO_3$ crystals in Gd_2O_3-Bi_2O_3-B_2O_3 glasses by YAG laser irradiation. *Appl. Phys. A* 89, 981–986. doi:10.1007/s00339-007-4200-9

Kozhayam, N., Ferriol, M., Cochez, M., and Aillerie, M. (2013). Growth and characterization of bismuth zinc borate $Bi_2ZnB_2O_7$ crystal fibers by the micro-pulling down technique. *J. Cryst. Growth* 364, 51–56. doi:10.1016/j.jcrysgro.2012.11.059

Liu, Z., Zeng, H., Ji, X., Ren, J., Chen, G., Ye, J., et al. (2015). Formation of $Bi_2ZnB_2O_7$ nanocrystals in ZnO-Bi_2O_3-B_2O_3 glass induced by femtosecond laser. *J. Am. Ceram. Soc.* 98, 408–412. doi:10.1111/jace.13330

Maeder, T. (2013). Review of Bi_2O_3 based glasses for electronics and related applications. *Int. Mater. Rev.* 58, 3–40. doi:10.1179/1743280412Y.0000000010

Majhi, K., and Varma, K. B. R. (2008a). Structural, dielectric and optical properties of transparent glasses and glass-ceramics of $SrBi_2B_2O_7$. *J. Non Cryst. Solids* 354, 4543–4549. doi:10.1016/j.jnoncrysol.2008.06.010

Majhi, K., and Varma, K. B. R. (2008b). Structural, dielectric and optical properties of $CaBi_2B_2O_7$ glasses and glass-nanocrystal composites. *Mater. Chem. Phys.* 117, 494–499. doi:10.1016/j.matchemphys.2009.06.044

Müller, R., Zanotto, E. D., and Fokin, V. M. (2000). Surface crystallization of silicate glasses: nucleation sites and kinetics. *J. Non Cryst. Solid*s 274, 208–231. doi:10.1016/S0022-3093(00)00214-3

Nishii, A., Shinozaki, K., Honma, T., and Komatsu, T. (2015). Morphology and orientation of β-BaB_2O_4 crystals patterned by laser in the inside of samarium barium borate glass. *J. Solid State Chem.* 221, 145–151. doi:10.1016/j.jssc.2014.09.031

Ogawa, K., Honma, T., and Komatsu, T. (2013). Birefringence imaging and orientation of laser patterned β-BaB_2O_4 crystals with bending and curved shapes in glass. *J. Solid State Chem.* 207, 6–12. doi:10.1016/j.jssc.2013.08.021

Sato, R., Benino, Y., Fujiwara, T., and Komatsu, T. (2001). YAG laser-induced crystalline dot patterning in samarium tellurite glasses. *J. Non Cryst. Solids* 289, 228–232. doi:10.1016/S0022-3093(01)00736-0

Shanmugavelu, B., and Kumar, V. V. R. K. (2012). Crystallization kinetics and phase transformation of bismuth zinc borate glass. *J. Am. Ceram. Soc.* 95, 2891–2898. doi:10.1111/j.1551-2916.2012.05342.x

Shinozaki, K., Honma, T., and Komatsu, T. (2012). New oxyfluoride glass with high fluorine content and laser patterning of nonlinear optical $BaAlBO_3F_2$ single crystal line. *J. Appl. Phys.* 112, 093506. doi:10.1063/1.4764326

Shinozaki, K., Noji, A., Honma, T., and Komatsu, T. (2013). Morphology and photoluminescence properties of Er^{3+}-doped CaF_2 nanocrystals patterned by laser irradiation in oxyfluoride glasses. *J. Fluor. Chem.* 145, 81–87. doi:10.1016/j.jfluchem.2012.10.007

Su, X., Wang, Y., Yang, Z., Huang, X. C., Pan, S., Li, F., et al. (2013). Experimental and theoretical studies on the linear and nonlinear optical properties of $Bi_2ZnOB_2O_6$. *J. Phys. Chem. C.* 117, 14149–14157. doi:10.1021/jp4013448

Suzuki, F., Honma, T., and Komatsu, T. (2010). Origin of periodic domain structure in Er^{3+}-doped β'-$(Sm,Gd)_2(MoO_4)_3$ crystal lines patterned by laser irradiations in glasses. *J. Solid State Chem.* 183, 909–914. doi:10.1016/j.jssc.2010.02.007

Terashima, K., Shimoto, T., and Yoko, T. (1997). Structure and nonlinear optical properties of PbO-Bi_2O_3-B_2O_3 glasses. *Phys. Chem. Glasses* 38, 211–217.

Tsukada, Y., Honma, T., and Komatsu, T. (2009). Self-organized periodic domain structure for second harmonic generation in ferroelastic β'-$(Sm,Gd)_2(MoO_4)_3$ crystal lines on glass surfaces. *Appl. Phys. Lett.* 94, 059901. doi:10.1063/1.3076080

Zeng, H., Liu, Z., Jiang, Q., Li, B., Yang, C., Shang, Z., et al. (2014). Large third-order optical nonlinearity of ZnO-Bi_2O_3-B_2O_3 glass-ceramic containing $Bi_2ZnB_2O_7$ nanocrystals. *J. Euro. Ceram. Soc.* 34, 4383–4388. doi:10.1016/j.jeurceramsoc.2014.06.031

Conflict of Interest Statement: The authors declare that the research was conducted in the absence of any commercial or financial relationships that could be construed as a potential conflict of interest.